

Cold-Atom Elevator: From Edge-State Injection to the Preparation of Fractional Chern Insulators

Botao Wang^{1,*}, Monika Aidelsburger^{1,2,3,4}, Jean Dalibard⁵, André Eckardt^{6,†} and Nathan Goldman^{1,5,‡}

¹CENOLI, Université Libre de Bruxelles, CP 231, Campus Plaine, B-1050 Brussels, Belgium

²Faculty of Physics, Ludwig-Maximilians-Universität München, Schellingstr. 4, D-80799 Munich, Germany

³Max-Planck-Institut für Quantenoptik, 85748 Garching, Germany

⁴Munich Center for Quantum Science and Technology (MCQST), Schellingstrasse 4, D-80799 Munich, Germany

⁵Laboratoire Kastler Brossel, Collège de France, CNRS, ENS-Université PSL, Sorbonne Université,
11 Place Marcelin Berthelot, 75005 Paris, France

⁶Technische Universität Berlin, Institut für Theoretische Physik, Hardenbergstrasse 36, 10623 Berlin, Germany



(Received 5 July 2023; accepted 12 March 2024; published 16 April 2024)

Optical box traps offer new possibilities for quantum-gas experiments. Building on their exquisite spatial and temporal control, we propose to engineer system-reservoir configurations using box traps, in view of preparing and manipulating topological atomic states in optical lattices. First, we consider the injection of particles from the reservoir to the system: this scenario is shown to be particularly well suited to activating energy-selective chiral edge currents, but also to prepare fractional Chern insulating ground states. Then, we devise a practical evaporative-cooling scheme to effectively cool down atomic gases into topological ground states. Our open-system approach to optical-lattice settings provides a new path for the investigation of ultracold quantum matter, including strongly correlated and topological phases.

DOI: 10.1103/PhysRevLett.132.163402

Introduction.—Optical box traps have been demonstrated as a powerful tool in cold-atom experiments [1]. Boxes of different shapes and dimensionalities have been realized for ultracold atoms or molecules [2–6], leading to the observation of the quantum Joule-Thomson effect [7] and recurrences in an isolated many-body system [8]; they also facilitated the detection of quantum depletion in atomic condensates [9], the low-energy spectrum of ultracold Fermi gases [10], and sound speed in superfluids [11–18]. Box traps have been used for state preparation, leading to the discovery of a novel breather in a 2D Bose gas [19], the deterministic preparation of a Townes soliton [20], and the demonstration of the transition between atomic and molecular condensates [21].

Combined with optical lattices, box potentials allow one to study a well-controlled number of atoms within a few lattice sites. This exquisite control opens up new possibilities, such as measuring entanglement growth upon a quench [22] or exploring the Fermi-Hubbard model [23–33] and many-body localization [34–36]. More recently, programmable box traps enabled the generation of large homogeneous lattice systems of more than 2000 atoms,

leading to large-scale quantum simulation of out-of-equilibrium dynamics [37–39]. In the context of topological matter, a Laughlin-type quantum Hall (QH) state has been realized with two strongly interacting bosons in a small box [40]. Isolating 1D lattices also allowed for the observation of the symmetry-protected Haldane phase [41] and 1D anyons [42]. The ability of creating optical boxes with sharp boundaries also offers an ideal framework to study topological edge modes [43,44].

Inspired by the possibility of shaping box potentials of arbitrary geometries, combined with the ability to control them dynamically, we propose to use box traps to partition a lattice system into different subregions, separating a “reservoir” region from a “system” of interest. We explore how dynamically tuning the relative energy between these two regions allows for the controlled preparation of interesting states within the system, a scheme coined “cold-atom elevator”; in practice, such a control is provided by digital micromirror devices and spatial light modulators [1]. We investigate two main scenarios: (i) injection of particles from the reservoir to the system, so as to populate edge states in an energy-resolved manner [Fig. 1(a)] or to prepare a strongly correlated topological ground state in the bulk [Fig. 1(b)]; (ii) controlled removal of particles from an excited state (e.g., a thermal metal), performed in a repeated “vacuum-cleaner” manner, in view of cooling the system down to a topological insulating ground state [Fig. 1(c)].

Edge-state injection.—A hallmark of topological matter, chiral edge states have been observed in photonic

Published by the American Physical Society under the terms of the [Creative Commons Attribution 4.0 International license](#). Further distribution of this work must maintain attribution to the author(s) and the published article’s title, journal citation, and DOI.

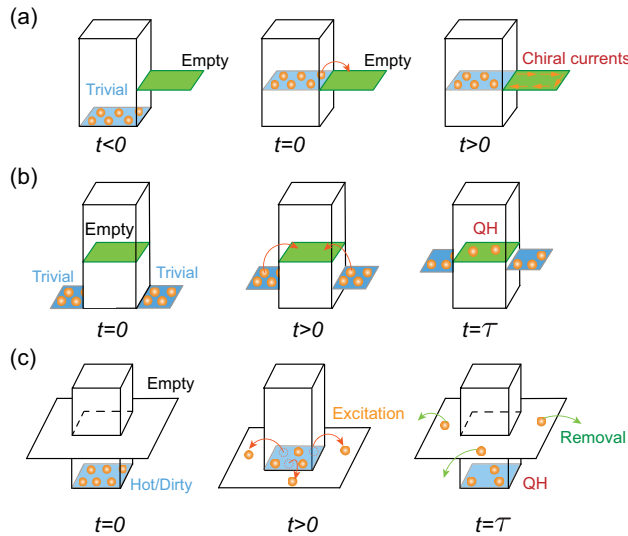


FIG. 1. The cold-atom elevator. (a) Protocol for chiral edge-state injection: setting the reservoir energy on resonance with the system’s edge modes, particles are continuously injected into edge states in an energy-selective manner, and chiral edge currents appear in the system without populating the bulk. (b) Injection protocol for state preparation: starting from a trivial state in the reservoirs, the latter are slowly lifted so as to adiabatically inject particles into the system until an insulating state, e.g., a quantum Hall state, is formed. (c) Cooling protocol for state preparation: a proper tuning of the reservoir energy can be used to retrieve excitations (hot atoms) from the system; removing the particles from the reservoir and repeating this lift-removal process over many cycles leads to the preparation of the desired insulating (QH) state in the system.

systems [45–47] and in cold atoms using synthetic dimensions [48–54]. Despite various proposals [55–62], the detection of real-space atomic chiral edge modes has only been reported recently [43,44]. We now show how our cold-atom elevator can activate topological edge currents within an empty system, in an energy-selective manner and without populating the bulk.

The general idea consists of coupling an empty lattice system, potentially hosting QH states, to a reservoir; see Fig. 1(a). Particles are initially prepared in the reservoir, in a state that can be chosen trivial [63]. We then perform a sudden lift of the reservoir energy ϵ_R to a proper value, such that the energy of the particles in the reservoir becomes resonant with the target edge mode in the system. In this way, energy-selective edge states will be populated in the initially empty system, allowing for the observation of chiral transport on a dark background.

As a concrete example, we consider the Harper-Hofstadter (HH) model [64], a square lattice with magnetic flux $\phi = 2\pi\alpha$ per plaquette, coupled to reservoirs,

$$\hat{H} = -\sum_{\langle \ell\ell' \rangle} (J_{\ell\ell'} e^{i\phi_{\ell\ell'}} \hat{a}_\ell^\dagger \hat{a}_{\ell'} + \text{H.c.}) + \sum_\ell \epsilon_\ell \hat{n}_\ell, \quad (1)$$

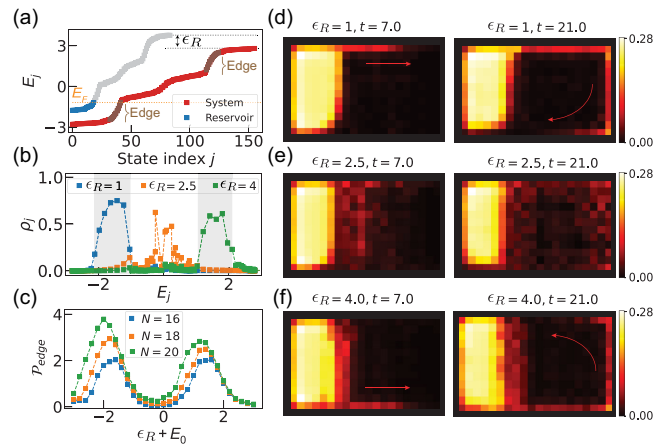


FIG. 2. Edge-state injection in the HH model. (a) Spectrum as a function of the eigenstate index j . The blue and red dots correspond to the Hamiltonian describing the reservoir (with $\epsilon_R = 1$) and the system, respectively; E_F is the Fermi energy. (b) Population of HH eigenstates ρ_j as a function of their energy E_j , at time $t = 28$. (c) Edge-mode population as a function of ϵ_R (compensated by E_0) for different initial particle number N in the reservoir. Snapshots of spatial density distribution for (d) $\epsilon_R = 1$, (e) $\epsilon_R = 2.5$, (f) $\epsilon_R = 4$ at times $t = 7, 21$. Here, a system of size 13×12 , with flux $\phi = \pi/2$ per plaquette, is coupled to a reservoir of size 7×12 . Except for (c), the number of particles is $N = 19$. Energy and time are in units of J and \hbar/J , respectively. The arrows in (d) and (f) are a guide to the eye for the chiral motion.

where $\hat{a}_\ell(\hat{a}_\ell^\dagger)$ are the annihilation (creation) operators on site ℓ and $\hat{n}_\ell = \hat{a}_\ell^\dagger \hat{a}_\ell$. We consider nearest-neighbor tunneling amplitudes $J_{\ell\ell'}$ and Peierls phases $\phi_{\ell\ell'}$ and set $\epsilon_\ell = \epsilon_R$ in the reservoir (zero otherwise). Box potentials are assumed to be sharp; smoothening effects are studied in the Supplemental Material [63]. Whether the reservoir is also subjected to the flux or not does not qualitatively change our findings [63]; here, we suppose that the entire system-reservoir setting is described by the HH model: we set $J_{\ell\ell'} = 1$ and choose Peierls phases $\phi_{\ell\ell'} = \phi n$ (respectively, 0) for hopping along x (respectively, y), where n is the lattice index along y .

The HH Hamiltonian is a paradigmatic model of Chern insulators (CIs): it hosts topologically nontrivial energy bands, which are characterized by nonzero Chern numbers [65]. Setting open boundary conditions, the model hosts chiral edge modes within the bulk energy gaps [58,59,63]. We show the energy spectrum for a system of size 13×12 and a reservoir of size 7×12 in Fig. 2(a); the regions of low density of states (steeper slopes), correspond to chiral edge states. When setting the reservoir energy to the value $\epsilon_R = 1$, the states populated in the reservoir become resonant with the chiral edge mode located in the lowest bulk gap of the system.

Based on this observation, we show how to populate edge states in an energy-selective manner. We start with

$N = 19$ particles in the reservoir, which corresponds to a complete filling of its nearly flat lowest Bloch band. We investigate the quench dynamics obtained by solving the time-dependent Schrödinger equation, using different values of ϵ_R . For $\epsilon_R = 1$, a clockwise chiral edge current is clearly observed in Fig. 2(d), where we plot the spatial density distribution at different times. When the box potential is lifted to $\epsilon_R = 4$, i.e., when the reservoir is resonant with the edge mode located in the upper bulk gap, an opposite chiral motion occurs [Fig. 2(f)]. Setting $\epsilon_R = 2.5$, the populated reservoir states are resonant with the system's middle Bloch band, in which case bulk states are populated in the system [Fig. 2(e)].

To quantify our edge-state injection scheme, we define the mean occupation $\rho_j(t)$ of an individual single-particle eigenstate j in the HH system. As shown in Fig. 2(b), we find dominant populations in the bulk gaps for $\epsilon_R = 1$ (lower gap) and $\epsilon_R = 4$ (upper gap). Furthermore, we define the total edge-state population $\mathcal{P}_{\text{edge}} = \sum_{j \in \text{edge}} \rho_j$, where the index j runs over all edge states. Figure 2(c) shows $\mathcal{P}_{\text{edge}}$ as a function of ϵ_R at time $t = 28$ for different particle numbers N . One observes a smaller edge-mode population when lowering the number of fermions in the reservoir. In any case, the peak positions clearly indicate the energy range of the edge (strong signal) and bulk (weak signal) modes. As a corollary, this scheme offers a spectroscopic tool for atomic QH systems [56–58,66].

FCI preparation based on particle injection.—A natural question concerns the possibility of using the injection scheme to form an insulating (QH) ground state within the bulk of the system. Here, we demonstrate the applicability of this scheme to realize a fractional Chern insulator (FCI): a lattice analog of a fractional QH state [67,68]. Several schemes have been proposed for realizing FCIs with cold atoms, based on the adiabatic variation of various system parameters [69–78]. Such a scheme was recently implemented to form an FCI state of two strongly interacting bosons in a 4×4 lattice [40]. We now show that an open-system approach, based on dynamically tuning box potentials, offers an alternative, potentially simpler, approach to prepare an FCI ground state with interacting bosons. The application to a CI of noninteracting fermions is studied in the Supplemental Material [63].

We consider the subbox configuration depicted in Fig. 1(b): the system is connected to two reservoirs (without flux). The initial state is an easily prepared trivial state with all (interacting) particles in the reservoirs. The system region, which is initially empty, is described by the Hofstadter-Bose-Hubbard model with hard-core interactions, which is known to host a $\nu = 1/2$ Laughlin-type ground state [79–84]. We aim at gently injecting particles from the reservoirs to the system, by slowly lifting the reservoirs' energy, in view of building up an FCI ground state in the system. Here, we set the hopping $J_{\ell\ell'} = J_R < 1$ within the reservoirs and the connecting interface, to limit excitations during preparation.

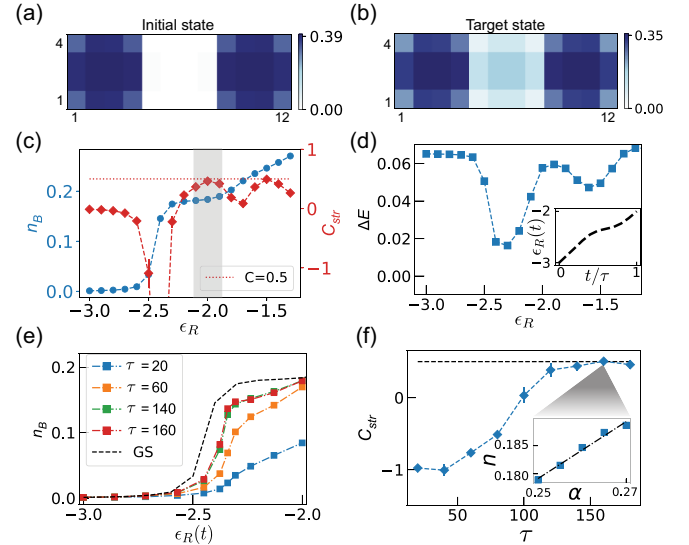


FIG. 3. Preparing an FCI based on injection. (a) Spatial density distribution of the initial state at $\epsilon_R = -3$. (b) Density distribution of the target state at $\epsilon_R = -2$. (c) Bulk density and the local Streda marker as a function of ϵ_R . The shadow indicates the FCI regime. (d) Many-body energy gap as a function of ϵ_R . Inset: the ramping protocol for $\epsilon_R(t)$ used in the next panels (e)–(f). (e) Bulk density as a function of ϵ_R for different τ and for the instantaneous ground state. (f) Streda marker as a function of τ . The dashed horizontal line indicates the ideal value $C_{\text{Str}} = 1/2$. Inset: linear fit of the density versus flux at $\tau = 160$, yielding $C_{\text{Str}} = 0.51$. Here, we consider $N = 12$ hard-core bosons; the system of size 4×4 is coupled to two reservoirs of size 4×4 , with $J_R = 0.15$. The error bars denote the standard error of the regression slope used to extract C_{Str} .

Calculations are performed using the density-matrix renormalization group method [85–89].

We first analyze the (static) ground-state properties of our system-reservoir setup, as a function of the reservoir energy ϵ_R ; see Figs. 3(a)–3(d). Figure 3(c) shows the bulk density n_B , as evaluated within the central 2×2 sites. The incompressible nature of the FCI state clearly manifests as a plateau in the bulk density. In contrast to more conventional closed-system schemes, the present system automatically chooses the ideal number of bosons to form the FCI state (for a given flux and number of lattice sites). The density reaches $n_B \approx 0.18$ on the plateau, and we verified that it converges toward the thermodynamic prediction $n_B = 1/8$ for increasing system sizes (up to 100 sites are considered in the Supplemental Material [63]). As another hallmark signature of the FCI, we evaluate the quantized Hall conductivity σ_H , which is encoded in the density distribution via Streda's formula [84,90–93],

$$C_{\text{Str}} = \frac{\partial n_B}{\partial \alpha} = \frac{\sigma_H}{\sigma_0}, \quad (2)$$

where $\sigma_0 = 1/2\pi$ is the conductivity quantum. For a $\nu = 1/2$ Laughlin state, the Streda marker is expected to

take the fractional value $C_{\text{Str}} = 1/2$, which is the many-body Chern number of the state. In our case, we find $C_{\text{Str}} \approx 0.46$ at $\epsilon_R = -2$, indicating the precursor of a fractional Hall response [Fig. 3(c)]. It is worth comparing this result with the value $C'_{\text{Str}} = 0.61$, which is obtained in the closed-box configuration of Ref. [40], where an exact number of bosons ($N = 2$) is loaded in 4×4 sites; this comparison supports the idea that the system optimizes the formation of an FCI state when coupled to reservoirs.

The bulk density and the Streda marker both show an interesting behavior across the transition that occurs as particles enter the system and eventually form the FCI state. Indeed, in the vicinity of $\epsilon_R \approx -2.5$, one notices an abrupt increase in n_B and a breakdown of Streda's formula [Fig. 3(c)], accompanied with a sudden drop in the many-body gap [Fig. 3(d)]. The minimal many-body gap associated with this transition is $\Delta = 0.016$, which suggests a realistic ramping time $\tau \sim 100$ for adiabatic preparation, compatible with recent experiments [40].

We now show that an FCI ground state can be dynamically prepared by slowly ramping up the reservoir energy to the ideal value $\epsilon_R \approx -2$. To optimize adiabatic preparation, we adjust the ramp according to the many-body gap; see inset in Fig. 3(d). By tracking the bulk density during the ramp [Fig. 3(e)], one recovers the formation of a plateau for a sufficiently long ramping time τ , in agreement with the adiabatic-limit prediction of Fig. 3(c). As further confirmed by the local Streda marker, an FCI ground state with $C_{\text{Str}} \approx 0.5$ is prepared for ramping times $\tau \gtrsim 140$ [Fig. 3(f)].

State preparation via repeated cleaning.—So far, we discussed protocols by which particles are injected from a reservoir into an empty system. Motivated by the ability of easily preparing an empty reservoir (a trivial zero-entropy state), we now explore the possibility of using this reservoir as a vacuum-cleaning resource to prepare ground states in the system. Starting from a “dirty” (excited) initial state within our system, the cleaning cycle is as follows [Fig. 1(c)]: (i) we slowly lower the reservoir energy, such as to retrieve excitations (hot atoms) from the system in a controlled manner; (ii) after this cleaning process, one rapidly lifts the reservoir until it becomes decoupled from the system, and one completely empties the reservoir. This cleaning cycle is then repeated N_{cyc} times, until convergence is reached toward a target insulating (QH) state in the system. The advantage of this scheme is twofold: the empty reservoir state can be viewed as a perfect and easy-to-prepare zero-temperature state of holes; the difficulty in removing particles that are located deep in the bulk is compensated by several repetitions; see also Refs. [94–97] on other cooling schemes based on engineered entropy transfer and thermalization.

We apply our repeated-cleaning scheme to a concrete preparation sequence, designed to prepare CIs in atomic HH systems. We start from a trivial metal realized by loading noninteracting fermions in a square lattice at half filling in the presence of a staggered potential [63]. As in

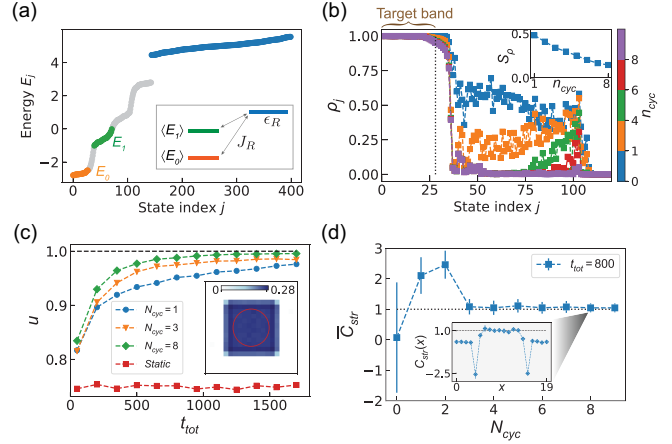


FIG. 4. Preparing a Chern insulator with a repeated-cleaning sequence. (a) Energy spectrum of the HH model coupled to a trivial reservoir. We partition a lattice of size 20×20 into a target 12×12 system (central box) and a surrounding reservoir; we set a flux $\phi = \pi/2$ in the system only. The aim is to empty the excited band E_1 , while keeping E_0 perfectly filled. Inset: simplified three-level model; $\langle E_0 \rangle$ and $\langle E_1 \rangle$ denote representative energies of the lowest two bands. (b) Population in HH eigenstates ρ_j , at various times $t = \tau n_{\text{cyc}}$, for $\tau = 100$ and $J_R = 0.15$. Inset: HH-orbital entropy versus n_{cyc} . (c) Uniformity factor as a function of the total cleaning time $t_{\text{tot}} = \tau N_{\text{cyc}}$, for different protocols (including a static evaporative scheme). The uniformity $u = 1 - \sqrt{\sum_{\ell} (n_{\ell} - \alpha)^2 / N_{\ell}}$ is evaluated in a central disk of radius $r = 4$ containing N_{ℓ} sites. Inset: density profile at the end of the sequence in (b). (d) The mean Streda marker \bar{C}_{Str} as a function of N_{cyc} , while fixing the total cleaning time ($t_{\text{tot}} = 800$); $N_{\text{cyc}} = 0$ corresponds to a static reservoir. The error bars reflect the Streda marker's standard deviation in the disk used in (c). Inset: local Streda marker along the central row at $N_{\text{cyc}} = 8$; the error bars reflect the standard error of the regression slope as in Fig. 3(f).

Ref. [98], we then ramp up the flux in the lattice to the value $\phi = \pi/2$, while reducing the staggered potential, hence changing the topological nature of the bands: at the end of this sequence, the target lowest band has a Chern number $C = 1$. Because of the occupation of higher bands in the initial metallic state, the target (lowest) band remains perfectly filled during the whole duration of the sequence, despite the gap closing ($C = 0 \rightarrow 1$). The irregular band populations, obtained at the end of this sequence, are shown by blue dots in Fig. 4(b).

Our aim is to remove atoms from higher bands, while leaving the lowest Chern band ($C = 1$) almost perfectly filled, in view of forming a CI in the system. To achieve this goal, we now apply our vacuum-cleaning protocol by dynamically tuning the reservoir energy ϵ_R . During each cycle of duration τ , we vary $\epsilon_R(t)$ with a saturation function [63], using a large initial value $\epsilon_R^i = 4$. At the end of this first cycle, $\epsilon_R(t)$ reaches the value $\epsilon_R^f = -1.14$, which is located right below the first excited Bloch band of the system. After lowering the reservoir to the final

value ϵ_R^f , we then quickly lift it up until it becomes effectively decoupled from the system; we then empty the reservoir and complete one cycle. We repeat this cleaning sequence N_{cyc} times, while increasing the final value ϵ_R^f at each cycle to properly address all the higher bands [63]. This cleaning scheme can be understood through a simplified three-level toy model [Fig. 4(a)], which can serve as a guide to optimize control parameters [63].

Figure 4(b) demonstrates the efficient depletion of the excited bands (and the resulting decrease of entropy) at successive steps of the sequence; $n_{\text{cyc}} = 1, \dots, N_{\text{cyc}}$ is the cycle index. The lowest band remains almost perfectly filled during the process, and we find that a satisfactory CI ground state is formed after $N_{\text{cyc}} = 8$ cycles of duration $\tau = 100$. We further characterize the state obtained at the end of the cleaning sequence by analyzing the uniformity of the particle density and the quantization of the Streda marker as a function of the total cleaning time t_{tot} and number of cycles N_{cyc} ; see Figs. 4(c) and 4(d). These results show that it is advantageous to consider several cycles ($N_{\text{cyc}} \sim 3\text{--}10$), and they highlight the advantage of our method over traditional evaporative schemes based on static reservoirs; see red squares in Fig. 4(c) and the Supplemental Material [63].

Concluding remarks.—This Letter explored different possibilities offered by the design of tunable boxes in cold-atom experiments, setting the focus on the realization of topological states. This approach offers substantial advantages: it relies on the preparation of a simple initial state in the reservoir and the ability to dynamically tune the latter's energy relative to the system region. In this sense, our open-system approach does not require complicated paths in parameter space, in contrast to the adiabatic-state-preparation schemes of Refs. [40,75–77]. It is readily applicable to create a broad class of many-body quantum states, including exotic Mott insulators and antiferromagnetic states in Hubbard-type models. While we considered a spatial separation between the system and reservoir regions on the 2D plane, we note that a double-layer configuration could also be envisaged to further enhance the transfer of particles between the two regions [63]; this could be realized using a bilayer optical lattice or by exploiting two laser-coupled internal states of an atom. Finally, it would be interesting to combine the injection and cleaning schemes presented in this Letter, in view of realizing large FCI states or to explore quantum thermodynamics.

The authors thank Julian Leonard, Yanfei Li, Nir Navon, Cecile Repellin, Raphael Saint-Jalm, Perrin Segura, Boye Sun, Amit Vashisht, and Christof Weitenberg for discussions. J. D. acknowledges the support of the Solvay Institutes, within the framework of the Jacques Solvay International Chairs in Physics. Density-matrix renormalization group

calculations were performed using the TeNPy library [89]. Work in Brussels is also supported by the FRS-FNRS (Belgium), the ERC Starting Grants TopoCold and LATIS, and the EOS project CHEQS. M. A. and A. E. acknowledge support from the Deutsche Forschungsgemeinschaft (DFG) via the Research Unit FOR 2414 under Project No. 277974659. M. A. also acknowledges funding from the DFG under Germany's Excellence Strategy—EXC-2111-390814868.

*botao.wang@ulb.be

†eckardt@tu-berlin.de

‡nathan.goldman@ulb.be

- [1] N. Navon, R. P. Smith, and Z. Hadzibabic, *Nat. Phys.* **17**, 1334 (2021).
- [2] A. L. Gaunt, T. F. Schmidutz, I. Gotlibovych, R. P. Smith, and Z. Hadzibabic, *Phys. Rev. Lett.* **110**, 200406 (2013).
- [3] L. Chomaz, L. Corman, T. Bienaimé, R. Desbuquois, C. Weitenberg, S. Nascimbene, J. Beugnon, and J. Dalibard, *Nat. Commun.* **6**, 6162 (2015).
- [4] B. Mukherjee, Z. Yan, P. B. Patel, Z. Hadzibabic, T. Yefsah, J. Struck, and M. W. Zwierlein, *Phys. Rev. Lett.* **118**, 123401 (2017).
- [5] K. Hueck, N. Luick, L. Sobirey, J. Siegl, T. Lompe, and H. Moritz, *Phys. Rev. Lett.* **120**, 060402 (2018).
- [6] R. Bause, A. Schindewolf, R. Tao, M. Duda, X.-Y. Chen, G. Quéméner, T. Karman, A. Christianen, I. Bloch, and X.-Y. Luo, *Phys. Rev. Res.* **3**, 033013 (2021).
- [7] T. F. Schmidutz, I. Gotlibovych, A. L. Gaunt, R. P. Smith, N. Navon, and Z. Hadzibabic, *Phys. Rev. Lett.* **112**, 040403 (2014).
- [8] B. Rauer, S. Erne, T. Schweigler, F. Cataldini, M. Tajik, and J. Schmiedmayer, *Science* **360**, 307 (2018).
- [9] R. Lopes, C. Eigen, N. Navon, D. Clément, R. P. Smith, and Z. Hadzibabic, *Phys. Rev. Lett.* **119**, 190404 (2017).
- [10] H. Biss, L. Sobirey, N. Luick, M. Bohlen, J. J. Kinnunen, G. M. Bruun, T. Lompe, and H. Moritz, *Phys. Rev. Lett.* **128**, 100401 (2022).
- [11] N. Navon, A. L. Gaunt, R. P. Smith, and Z. Hadzibabic, *Nature (London)* **539**, 72 (2016).
- [12] J. L. Ville, R. Saint-Jalm, E. Le Cerf, M. Aidelsburger, S. Nascimbène, J. Dalibard, and J. Beugnon, *Phys. Rev. Lett.* **121**, 145301 (2018).
- [13] L. Baird, X. Wang, S. Roof, and J. E. Thomas, *Phys. Rev. Lett.* **123**, 160402 (2019).
- [14] P. B. Patel, Z. Yan, B. Mukherjee, R. J. Fletcher, J. Struck, and M. W. Zwierlein, *Science* **370**, 1222 (2020).
- [15] M. Bohlen, L. Sobirey, N. Luick, H. Biss, T. Enss, T. Lompe, and H. Moritz, *Phys. Rev. Lett.* **124**, 240403 (2020).
- [16] S. J. Garratt, C. Eigen, J. Zhang, P. Turzák, R. Lopes, R. P. Smith, Z. Hadzibabic, and N. Navon, *Phys. Rev. A* **99**, 021601(R) (2019).
- [17] P. Christodoulou, M. Gałka, N. Dogra, R. Lopes, J. Schmitt, and Z. Hadzibabic, *Nature (London)* **594**, 191 (2021).
- [18] J. Zhang, C. Eigen, W. Zheng, J. A. P. Glidden, T. A. Hilker, S. J. Garratt, R. Lopes, N. R. Cooper, Z. Hadzibabic, and N. Navon, *Phys. Rev. Lett.* **126**, 060402 (2021).

- [19] R. Saint-Jalm, P. C. M. Castilho, E. Le Cerf, B. Bakkali-Hassani, J.-L. Ville, S. Nascimbene, J. Beugnon, and J. Dalibard, *Phys. Rev. X* **9**, 021035 (2019).
- [20] B. Bakkali-Hassani, C. Maury, Y.-Q. Zou, E. Le Cerf, R. Saint-Jalm, P. C. M. Castilho, S. Nascimbene, J. Dalibard, and J. Beugnon, *Phys. Rev. Lett.* **127**, 023603 (2021).
- [21] Z. Zhang, L. Chen, K.-X. Yao, and C. Chin, *Nature (London)* **592**, 708 (2021).
- [22] R. Islam, R. Ma, P. M. Preiss, M. E. Tai, A. Lukin, M. Rispoli, and M. Greiner, *Nature (London)* **528**, 77 (2015).
- [23] A. Mazurenko, C. S. Chiu, G. Ji, M. F. Parsons, M. Kanász-Nagy, R. Schmidt, F. Grusdt, E. Demler, D. Greif, and M. Greiner, *Nature (London)* **545**, 462 (2017).
- [24] C. S. Chiu, G. Ji, A. Mazurenko, D. Greif, and M. Greiner, *Phys. Rev. Lett.* **120**, 243201 (2018).
- [25] M. A. Nichols, L. W. Cheuk, M. Okan, T. R. Hartke, E. Mendez, T. Senthil, E. Khatami, H. Zhang, and M. W. Zwierlein, *Science* **363**, 383 (2019).
- [26] P. T. Brown, D. Mitra, E. Guardado-Sánchez, R. Nourafkan, A. Reymbaut, C.-D. Hébert, S. Bergeron, A.-M. Tremblay, J. Kokalj, D. A. Huse *et al.*, *Science* **363**, 379 (2019).
- [27] C. S. Chiu, G. Ji, A. Bohrdt, M. Xu, M. Knap, E. Demler, F. Grusdt, M. Greiner, and D. Greif, *Science* **365**, 251 (2019).
- [28] J. Koepsell, J. Vijayan, P. Sompel, F. Grusdt, T. A. Hilker, E. Demler, G. Salomon, I. Bloch, and C. Gross, *Nature (London)* **572**, 358 (2019).
- [29] T. Hartke, B. Oreg, N. Jia, and M. Zwierlein, *Phys. Rev. Lett.* **125**, 113601 (2020).
- [30] J. Vijayan, P. Sompel, G. Salomon, J. Koepsell, S. Hirthe, A. Bohrdt, F. Grusdt, I. Bloch, and C. Gross, *Science* **367**, 186 (2020).
- [31] M. Gall, N. Wurz, J. Samland, C. F. Chan, and M. Köhl, *Nature (London)* **589**, 40 (2021).
- [32] S. Hirthe, T. Chalopin, D. Bourgund, P. Bojović, A. Bohrdt, E. Demler, F. Grusdt, I. Bloch, and T. A. Hilker, *Nature (London)* **613**, 463 (2023).
- [33] M. Xu, L. H. Kendrick, A. Kale, Y. Gang, G. Ji, R. T. Scalettar, M. Lebrat, and M. Greiner, *Nature (London)* **620**, 971 (2023).
- [34] A. Lukin, M. Rispoli, R. Schittko, M. E. Tai, A. M. Kaufman, S. Choi, V. Khemani, J. Leonard, and M. Greiner, *Science* **364**, 256 (2019).
- [35] M. Rispoli, A. Lukin, R. Schittko, S. Kim, M. E. Tai, J. Léonard, and M. Greiner, *Nature (London)* **573**, 385 (2019).
- [36] J. Léonard, S. Kim, M. Rispoli, A. Lukin, R. Schittko, J. Kwan, E. Demler, D. Sels, and M. Greiner, *Nat. Phys.* **19**, 481 (2023).
- [37] D. Wei, A. Rubio-Abadal, B. Ye, F. Machado, J. Kemp, K. Srakaew, S. Hollerith, J. Rui, S. Gopalakrishnan, N. Y. Yao *et al.*, *Science* **376**, 716 (2022).
- [38] A. Impertro, J. F. Wienand, S. Häfele, H. von Raven, S. Hubele, T. Klostermann, C. R. Cabrera, I. Bloch, and M. Aidelsburger, *Commun. Phys.* **6**, 166 (2023).
- [39] J. F. Wienand, S. Karch, A. Impertro, C. Schweizer, E. McCulloch, R. Vasseur, S. Gopalakrishnan, M. Aidelsburger, and I. Bloch, *arXiv:2306.11457*.
- [40] J. Léonard, S. Kim, J. Kwan, P. Segura, F. Grusdt, C. Repellin, N. Goldman, and M. Greiner, *Nature (London)* **619**, 495 (2023).
- [41] P. Sompel, S. Hirthe, D. Bourgund, T. Chalopin, J. Bibo, J. Koepsell, P. Bojović, R. Verresen, F. Pollmann, G. Salomon *et al.*, *Nature (London)* **606**, 484 (2022).
- [42] J. Kwan, P. Segura, Y. Li, S. Kim, A. V. Gorshkov, A. Eckardt, B. Bakkali-Hassani, and M. Greiner, *arXiv:2306.01737*.
- [43] C. Braun, R. Saint-Jalm, A. Hesse, J. Arceri, I. Bloch, and M. Aidelsburger, *arXiv:2304.01980*.
- [44] R. Yao, S. Chi, B. Mukherjee, A. Shaffer, M. Zwierlein, and R. J. Fletcher, *arXiv:2304.10468*.
- [45] M. C. Rechtsman, J. M. Zeuner, Y. Plotnik, Y. Lumer, D. Podolsky, F. Dreisow, S. Nolte, M. Segev, and A. Szameit, *Nature (London)* **496**, 196 (2013).
- [46] M. Hafezi, S. Mittal, J. Fan, A. Migdall, and J. Taylor, *Nat. Photonics* **7**, 1001 (2013).
- [47] T. Ozawa, H. M. Price, A. Amo, N. Goldman, M. Hafezi, L. Lu, M. C. Rechtsman, D. Schuster, J. Simon, O. Zilberberg, and I. Carusotto, *Rev. Mod. Phys.* **91**, 015006 (2019).
- [48] M. Mancini, G. Pagano, G. Cappellini, L. Livi, M. Rider, J. Catani, C. Sias, P. Zoller, M. Inguscio, M. Dalmonte, and L. Fallani, *Science* **349**, 1510 (2015).
- [49] B. K. Stuhl, H.-I. Lu, L. M. Aycock, D. Genkina, and I. B. Spielman, *Science* **349**, 1514 (2015).
- [50] L. F. Livi, G. Cappellini, M. Diem, L. Franchi, C. Clivati, M. Frittelli, F. Levi, D. Calonico, J. Catani, M. Inguscio, and L. Fallani, *Phys. Rev. Lett.* **117**, 220401 (2016).
- [51] F. A. An, E. J. Meier, and B. Gadway, *Sci. Adv.* **3**, e1602685 (2017).
- [52] E. Lustig, S. Weimann, Y. Plotnik, Y. Lumer, M. A. Bandres, A. Szameit, and M. Segev, *Nature (London)* **567**, 356 (2019).
- [53] T. Chalopin, T. Satoor, A. Evrard, V. Makhalov, J. Dalibard, R. Lopes, and S. Nascimbene, *Nat. Phys.* **16**, 1017 (2020).
- [54] T. Ozawa and H. M. Price, *Nat. Rev. Phys.* **1**, 349 (2019).
- [55] N. Goldman, I. Satija, P. Nikolic, A. Bermudez, M. A. Martin-Delgado, M. Lewenstein, and I. B. Spielman, *Phys. Rev. Lett.* **105**, 255302 (2010).
- [56] T. D. Stanescu, V. Galitski, and S. Das Sarma, *Phys. Rev. A* **82**, 013608 (2010).
- [57] X.-J. Liu, X. Liu, C. Wu, and J. Sinova, *Phys. Rev. A* **81**, 033622 (2010).
- [58] N. Goldman, J. Beugnon, and F. Gerbier, *Phys. Rev. Lett.* **108**, 255303 (2012).
- [59] N. Goldman, J. Dalibard, A. Dauphin, F. Gerbier, M. Lewenstein, P. Zoller, and I. B. Spielman, *Proc. Natl. Acad. Sci. U.S.A.* **110**, 6736 (2013).
- [60] M. D. Reichl and E. J. Mueller, *Phys. Rev. A* **89**, 063628 (2014).
- [61] N. Goldman, G. Jotzu, M. Messer, F. Görg, R. Desbuquois, and T. Esslinger, *Phys. Rev. A* **94**, 043611 (2016).
- [62] B. Wang, F. N. Ünal, and A. Eckardt, *Phys. Rev. Lett.* **120**, 243602 (2018).
- [63] See Supplemental Material at <http://link.aps.org/supplemental/10.1103/PhysRevLett.132.163402> for the Harper-Hofstadter band structure; further informations regarding the edge-state injection, and the preparation of (fractional) Chern insulators; details on the repeated-cleaning scheme; comparison between particle-injection and repeated-cleaning methods.
- [64] D. R. Hofstadter, *Phys. Rev. B* **14**, 2239 (1976).

- [65] N. R. Cooper, J. Dalibard, and I. B. Spielman, *Rev. Mod. Phys.* **91**, 015005 (2019).
- [66] Q. Liang, D. Xie, Z. Dong, H. Li, H. Li, B. Gadway, W. Yi, and B. Yan, *Phys. Rev. Lett.* **129**, 070401 (2022).
- [67] E. J. Bergholtz and Z. Liu, *Int. J. Mod. Phys. B* **27**, 1330017 (2013).
- [68] S. A. Parameswaran, R. Roy, and S. L. Sondhi, *C.R. Phys.* **14**, 816 (2013).
- [69] M. Popp, B. Paredes, and J. I. Cirac, *Phys. Rev. A* **70**, 053612 (2004).
- [70] N. Y. Yao, A. V. Gorshkov, C. R. Laumann, A. M. Läuchli, J. Ye, and M. D. Lukin, *Phys. Rev. Lett.* **110**, 185302 (2013).
- [71] E. Kapit, M. Hafezi, and S. H. Simon, *Phys. Rev. X* **4**, 031039 (2014).
- [72] F. Grusdt, F. Letscher, M. Hafezi, and M. Fleischhauer, *Phys. Rev. Lett.* **113**, 155301 (2014).
- [73] M. Barkeshli, N. Y. Yao, and C. R. Laumann, *Phys. Rev. Lett.* **115**, 026802 (2015).
- [74] C. Repellin, T. Yefsah, and A. Sterdyniak, *Phys. Rev. B* **96**, 161111(R) (2017).
- [75] J. Motruk and F. Pollmann, *Phys. Rev. B* **96**, 165107 (2017).
- [76] Y.-C. He, F. Grusdt, A. Kaufman, M. Greiner, and A. Vishwanath, *Phys. Rev. B* **96**, 201103(R) (2017).
- [77] A. Hudomal, N. Regnault, and I. Vasić, *Phys. Rev. A* **100**, 053624 (2019).
- [78] B. Andrade, V. Kasper, M. Lewenstein, C. Weitenberg, and T. Graß, *Phys. Rev. A* **103**, 063325 (2021).
- [79] A. S. Sørensen, E. Demler, and M. D. Lukin, *Phys. Rev. Lett.* **94**, 086803 (2005).
- [80] M. Hafezi, A. S. Sørensen, E. Demler, and M. D. Lukin, *Phys. Rev. A* **76**, 023613 (2007).
- [81] M. Gerster, M. Rizzi, P. Silvi, M. Dalmonte, and S. Montangero, *Phys. Rev. B* **96**, 195123 (2017).
- [82] P. Rosson, M. Lubasch, M. Kiffner, and D. Jaksch, *Phys. Rev. A* **99**, 033603 (2019).
- [83] B. Wang, X.-Y. Dong, and A. Eckardt, *SciPost Phys.* **12**, 095 (2022).
- [84] C. Repellin, J. Léonard, and N. Goldman, *Phys. Rev. A* **102**, 063316 (2020).
- [85] S. R. White, *Phys. Rev. Lett.* **69**, 2863 (1992).
- [86] U. Schollwöck, *Rev. Mod. Phys.* **77**, 259 (2005).
- [87] M. P. Zaletel, R. S. K. Mong, C. Karrasch, J. E. Moore, and F. Pollmann, *Phys. Rev. B* **91**, 165112 (2015).
- [88] M. Gohlke, R. Verresen, R. Moessner, and F. Pollmann, *Phys. Rev. Lett.* **119**, 157203 (2017).
- [89] J. Hauschild and F. Pollmann, *SciPost Phys. Lect. Notes* **5** (2018).
- [90] A. Widom, *Phys. Lett.* **90A**, 474 (1982).
- [91] P. Streda, *J. Phys. C* **15**, L717 (1982).
- [92] P. Streda and L. Smrcka, *J. Phys. C* **16**, L895 (1983).
- [93] R. O. Umucalilar, H. Zhai, and M. O. Oktel, *Phys. Rev. Lett.* **100**, 070402 (2008).
- [94] J. I. Cirac and M. Lewenstein, *Phys. Rev. A* **52**, 4737 (1995).
- [95] T.-L. Ho and Q. Zhou, *Proc. Natl. Acad. Sci. U.S.A.* **106**, 6916 (2009).
- [96] J.-S. Bernier, C. Kollath, A. Georges, L. De Leo, F. Gerbier, C. Salomon, and M. Köhl, *Phys. Rev. A* **79**, 061601(R) (2009).
- [97] B. Yang, H. Sun, C.-J. Huang, H.-Y. Wang, Y. Deng, H.-N. Dai, Z.-S. Yuan, and J.-W. Pan, *Science* **369**, 550 (2020).
- [98] M. Aidelsburger, M. Lohse, C. Schweizer, M. Atala, J. T. Barreiro, S. Nascimbène, N. Cooper, I. Bloch, and N. Goldman, *Nat. Phys.* **11**, 162 (2015).